THE JOURNAL OF BIOLOGICAL CHEMISTRY
Vol. 257, No. 9, Issue of May 10, pp. 5023-5029, 1982
Printed in U.S.A.

Nuclear Magnetic Resonance of Hemeprotein Crystals

STRUCTURE OF THE HEME IN *PHYSETER CATODON* FERRIMYOGLOBIN AND AN ANALYSIS OF HYPERFINE SHIFTS*

(Received for publication, September 14, 1981)

Robert W. K. Lee and Eric Oldfield‡

From the School of Chemical Sciences, University of Illinois at Urbana-Champaign, Urbana, Illinois 61801

We report the observation of deuterium Fourier transform NMR spectra (obtained by the quadrupole echo method at 8.5 Tesla, corresponding to a ^2H resonance frequency of 55.3 MHz) of [*meso*-α,β,γ,δ-$^2H_4$], [*methyl*-1,3-$^2H_6$], and [*methylene*-6,7-*b*-$^2H_4$]heme-labeled aquoferrimyoglobin microcrystals (in ~90% saturated $(NH_4)_2SO_4$ at pH 6.8) from *Physeter catodon*, using the method of magnetic ordering (Rothgeb, T. M., and Oldfield, E. (1981) *J. Biol. Chem.* 256, 1432-1446). The results, together with those obtained on suitable diamagnetic derivatives, permit partial determination of the static organization of the heme, and the results obtained are in good agreement with those obtained using x-ray crystallography (Takano, T. (1977) *J. Mol. Biol.* 110, 537-568). We show that resonances near the paramagnetic iron center are subject to extremely large (~500 ppm) hyperfine shifts, which distort the otherwise symmetric ^2H spectra. Temperature dependence studies are required to analyze these shifts, which are an order of magnitude larger than those seen in solution NMR spectroscopy. The overall results suggest that ^2H solid state NMR spectroscopy of magnetically ordered paramagnetic protein microcrystals may be a useful method for determination of heme organization in systems that for one reason or another are unsuitable for analysis using x-ray diffraction methods.

Two of the most powerful physical methods available today for investigating the static and dynamic structures of proteins (or more generally speaking biological macromolecules) are x-ray crystallography (1) and nuclear magnetic resonance spectroscopy (2-6). X-ray diffraction gives, of course, the most direct static structural information, but despite the continual advances in instrumentation and technique, many proteins cannot be studied crystallographically due to the lack of suitable crystal forms. NMR spectroscopy in solution is not plagued by the problems of having suitable crystals (only suitable quantities), but solution NMR results only give static structural information indirectly. By contrast, NMR spectroscopy in solution gives in a fairly direct fashion information that may be interpreted in dynamical terms (7), information that is less readily available to the crystallographic methods (8, 9). In order to complement both methods, we have, therefore, recently developed the method of magnetic ordering (10-12) which permits resolution of individual sites in suitably labeled protein crystals and, thereby, permits study of their static and dynamic properties. In this paper, we outline our progress with the method in determining the static organization of the heme ring in ferriaquomyoglobin microcrystals from sperm whale (*Physeter catodon*) in order to show that the method may in the future have some utility in determining the orientations of various groups in some proteins that seem to be immune to crystallization.

* This work was supported by United States National Institutes of Health Grant HL-19481, by equipment Grants PCM 78-23021 and PCM 79-23170 provided by the United States National Science Foundation, by the Alfred P. Sloan Foundation, the American Heart Association (Grant 80-867), and has benefitted by use of equipment made available through the University of Illinois-National Science Foundation Regional Instrumentation Facility Grant CHE 79-16100. The costs of publication of this article were defrayed in part by the payment of page charges. This article must therefore be hereby marked "*advertisement*" in accordance with 18 U.S.C. Section 1734 solely to indicate this fact.

‡ Alfred P. Sloan Research Fellow 1978-1980; United States Public Health Service Research Career Development Awardee, 1979-1984 (Grant CA-00595).

EXPERIMENTAL PROCEDURES

Synthesis of ^2H-labeled Hemes

[Meso-α,β,γ,δ-$^2H_4$]protoporphyrin IX Dimethyl Ester—Protoporphyrin IX dimethyl ester from ox heme was obtained from Sigma and used without further purification. The deuteration of the meso-α, β, γ, and δ positions of the protoporphyrin macrocycle (Fig. 1) was achieved using procedures similar to those described for deuteration of the meso-positions of coproporphyrin I tetramethyl ester (13). 800 mg of Mg powder, 1.5 g of I_2, and 30 ml of diethyl ether were refluxed under nitrogen until colorless (about 30 min). Excess Mg was filtered off, and the solution evaporated to dryness under reduced pressure. The residual yellow solid was dissolved in 50 ml of pyridine containing 2 ml of [*O*-$^2H_1$]methanol. In a typical deuteration, 20 ml of this solution were then added to ~150 mg of protoporphyrin IX dimethyl ester dissolved in a minimum amount of dry pyridine. The resulting solution was refluxed under nitrogen for 4 h. After cooling, 50 ml of $CHCl_3$ were added and the mixture poured into 200 ml of 3% citric acid. The organic layer was washed three times with water and then dried over Na_2SO_4. Solvent was removed under reduced pressure and the residue was set aside overnight in 200 ml of 5% sulfuric acid in methanol. This solution was then poured into water, and the protoporphyrin IX dimethyl ester extracted with chloroform, washed with water, and finally dried over Na_2SO_4. The residue after solvent removal was chromatographed on alumina (Woelm neutral, grade V) using CH_2Cl_2. A minimum amount of methylene chloride and excess methanol, or *n*-hexane, was used to crystallize the pure [*meso*-α,β,γ,δ-$^2H_4$]protoporphyrin IX dimethyl ester. The yield was about 80%. Meso-deuterated protoporphyrin synthesized by a similar method (14) indicated 50% deuteration of the β-methylene protons of the vinyl groups. However, ^1H NMR data (at 220 MHz) on our product indicated that it is essentially free from such unwanted substitution, and comparison with the proton magnetic resonance spectra of protoporphyrin IX dimethyl ester reported in Ref. 15 indicates that about 80% deuteration was achieved at the meso-α, β, γ, and δ positions.

[Methylene-6,7-b-$^2H_4$]protoporphyrin IX Dimethyl Ester—To a warmed solution of 200 mg of protoporphyrin IX dimethyl ester in 200 ml of dimethylformamide were added 10 ml of a 0.25 M solution of freshly prepared sodium methoxide in CH_3O^2H. The solution was allowed to stand until a bulky purplish precipitate appeared, then 100 ml of $CHCl_3$ were added, and the mixture poured into 200 ml of 3% citric acid. Further work-up was the same as that described above.

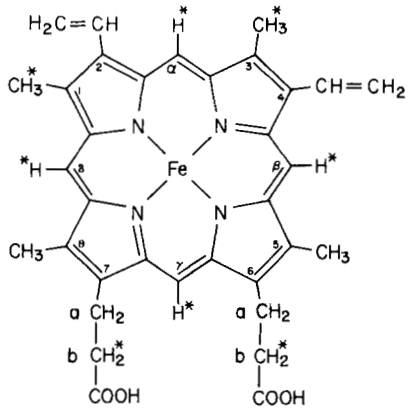

FIG. 1. Structure of the heme moiety of myoglobin showing numbering scheme and position of deuterium labels.

The yield was about 70–80%. All four protons were completely exchanged as determined by ^{1}H NMR spectroscopy (at 220 MHz).

[Dimethyl-1,3-$^2H_6$]protoporphyrin IX Dimethyl Ester—There are two published synthetic routes for this compound (16, 17). The method in Ref. 16 in our hands yielded a 50% deuterated material, which was useful in spectral assignment as discussed under "Results and Discussion." The second method (17) involved a six-step synthesis and gave a product containing 80% deuteration in the 1,3-methyl groups, together with a 100% deuteration of the 6,7-*b*-methylene groups. ^{2}H NMR results were obtained on protein microcrystals containing both labeled hemes and on a 6,7-*b*-methylene back-exchanged sample as discussed below.

Formation of Deuterated Protohemin—In order to minimize the possibility of back exchange of ^{2}H, we used an iron insertion method basically as described by Adler *et al.* (18). One hundred mg of deuterated protoporphyrin IX dimethyl ester were dissolved in 100 ml of dimethylformamide, and the solution refluxed for 1 min. The stoichiometric amount of $FeCl_2$ was then added and the solution refluxed for 20 min. Iron insertion was followed spectrophotometrically. After cooling on ice for 15 min, 300–400 ml of cold water were added to precipitate the protohemin dimethyl ester. The precipitate was centrifuged and dried over P_4O_{10}. The yield was approximately 90%. Hydrolysis of the ester functional group was effected using a solution containing 3% KOH, 5% ^2H_2O, and 92% CH_3O^2H at 70 °C for 1 h. Deuterated solvents were used except in the case of meso-$^2H_4$-labeled protoporphyrin IX dimethyl ester. The resulting protohemins were precipitated by addition of acetic acid and a saturated NaCl solution followed by centrifugation. Protohemin purity was estimated spectrophotometrically as the pyridine hemochromogen. Per cent deuteration was determined by 220 MHz ^{1}H NMR spectroscopy of the putative biscyano complex (19).

Apomyoglobin and Reconstitution Method—Sperm whale myoglobin was obtained from Sigma and purified according to Hapner *et al.* (20). Apomyoglobin was typically prepared by taking 200 ml of a 2% solution of purified protein at pH 3.5, in the presence of 0.1 M NaF, and using 2-butanone for heme extraction. The yield was usually about 50% (21). The apomyoglobin was extensively dialyzed against distilled, deionized water to remove 2-butanone and stored in lyophilized form at −20 °C.

Apomyoglobin was re-hemed by adding 38 mg of protohemin (in 0.05 M NaOH) to 1 g of apomyoglobin (11, 21), followed by stirring for 10 min at 4 °C. The resulting solutions were dialyzed until the pH dropped to ~8.0. The solutions were then concentrated by ultrafiltration and then brought to pH 6.35 with KH_2PO_4. Small amounts of precipitate were removed by centrifugation, and the brown solutions chromatographed on CM-50 Sephadex, equilibrated, and eluted with pH 6.5 phosphate buffer at 0.1 ionic strength. Reconstituted myoglobins separated from "denatured" myoglobins, which remained at the top of the column after 3–4 h (11). Eluted myoglobin was concentrated by ultrafiltration, deionized on freshly washed Rexyn I-300 (Fisher), and crystallized immediately. For crystallization, 2–4% solutions of labeled aquoferrimyoglobin were slowly mixed with saturated $(NH_4)_2SO_4$ buffered at pH 6.35. At ~60% $(NH_4)_2SO_4$ saturation, a precipitate formed, which was removed by Millipore filtration. The solutions were then brought to 70% $(NH_4)_2SO_4$ saturation and placed into silylated glass vials for crystallization. Crystals were obtained after about 1 week and were of the monoclinic type belonging to space group $P2_1$ (22).

Nuclear Magnetic Resonance Spectroscopy

Two "home built" Fourier transform NMR spectrometers were used to record spectra. The first one used an 8.5 Tesla 3.5-inch bore high resolution superconducting solenoid (Oxford Instruments, Osney Mead, Oxford, England) together with a variety of digital and radiofrequency electronics. We used a Nicolet (Madison, WI) model 1180 computer, 293B pulse programmer, NIC-2090 dual channel 50-ns transient recorder for rapid data acquisition, and a Diablo model 40 disc system for data storage (Diablo Systems, Inc., Hayward, CA). In order to generate high enough power radiofrequency pulses to cover the entire ^{2}H spectral breadth, we used an Amplifier Research (Souderton, PA) model 200L amplifier to drive a retuned Henry Radio (Los Angeles, CA) model 2006 transmitter to an approximately 1000–1500-watt output power level. Additional ^{2}H spectra were recorded using the 5.2 Tesla wide bore system described previously (23). NMR samples were prepared by first removing excess 70% saturated $(NH_4)_2SO_4$ by filtration, followed by resuspension of microcrystals in ~100% saturated $(NH_4)_2SO_4$ solution in ^{2}H-depleted H_2O (Aldrich), the pH being adjusting using phosphate buffer. Spectra were recorded using 100–200 mg of microcrystals with a quadrupole echo pulse sequence (90°_x-τ_1-90°_y-τ_2; Ref. 24). The 90° pulse width was generally 2.5–3.5 μs at 8.5 Tesla and ~7 μs at 5.2 Tesla.

Spectral Simulations—Spectral simulations were carried out on the University of Illinois Digital Computer Laboratory's Control Data Corp. Cyber-175 system, which is interfaced to a Tektronix 4006 graphics terminal and Tektronix 4662 interactive digital plotter (Tektronix, Beaverton, OR) in our laboratory, as described previously (11).

Theoretical Aspects

The general theoretical background appropriate for discussion of the ^{2}H NMR spectra of magnetically ordered proteins is discussed in a previous paper (11). However, in the case of ^{2}H-labeled hemes, the complete Hamiltonian will be more complex than described before due to the proximity of the paramagnetic center. Consequently, we have

$$\mathcal{H} = \mathcal{H}_Z + \mathcal{H}_Q + \mathcal{H}_{DD} + \mathcal{H}_{CSA} + \mathcal{H}_{SC} + \mathcal{H}_F + \mathcal{H}_D + \mathcal{H}_L \quad (1)$$

where $\mathcal{H}_Z$, $\mathcal{H}_Q$, $\mathcal{H}_{DD}$, $\mathcal{H}_{CSA}$, $\mathcal{H}_{SC}$, $\mathcal{H}_F$, $\mathcal{H}_D$, and $\mathcal{H}_L$ represent the nuclear Zeeman, quadrupole, dipole-dipole, chemical shift, scalar coupling, Fermi contact, electron-nuclear dipolar, and orbital interactions, respectively. The important point to note is that there will potentially be large shifts due to the addition of the last three terms in Equation 1 for nuclei near the paramagnetic heme iron. A detailed discussion of these new terms is given elsewhere (25, 26), but for our purposes, we feel it is useful to quote a few results. First, we note that it is possible to write the resonance shifts as a function of principal components of the magnetic susceptibility tensor (26)

$$\left(\frac{\Delta H}{H}\right)^{D+L} = \frac{1}{2R^3}\left\{(1-3\cos^2\theta)\left(\frac{2}{3}\chi_{zz} - \frac{1}{3}\chi_{xx} - \frac{1}{3}\chi_{yy}\right) + \sin^2\theta\cos 2\Omega\,(\chi_{yy} - \chi_{xx})\right\} \quad (2)$$

$$\left(\frac{\Delta H}{H}\right)^{F} = -\frac{a_N}{6\hbar\gamma_N\beta}\left\{\frac{\chi_{xx}g_{S_{xx}}}{g_{xx}} + \frac{\chi_{yy}g_{S_{yy}}}{g_{yy}} + \frac{\chi_{zz}g_{S_{zz}}}{g_{zz}}\right\} \quad (3)$$

where $(\Delta H/H)$ are the fractional resonance shifts, θ is the angle between σ and the z axis, Ω is the angle between the x axis and the projection of σ in the xy plane, R is the distance from the paramagnetic center, χ_{xx}, χ_{yy}, and χ_{zz} are the principal components of the magnetic susceptibility tensor, and a_N is the Fermi contact coupling constant. For the simple case of no zero field splitting,

$$\chi_{ii} = [g_{ii}^2\beta^2 s'(s'+1)]/3kT \quad (4)$$

the dipolar shift is

$$\left(\frac{\Delta H}{H}\right)^{D+L} = \frac{\beta^2 s'(s'+1)}{18kTR^3}\{[2g_{zz}^2 - (g_{xx}^2 + g_{yy}^2)] \cdot (1-3\cos^2\theta) + 3(g_{yy}^2 - g_{xx}^2)\sin^2\theta\cos 2\Omega\} \quad (5)$$

and the contact shift is

$$\left(\frac{\Delta H}{H}\right)^{F} = -\frac{a_N \beta s'(s'+1)}{6\hbar\gamma_N kT}\left[\frac{g_{xx}g_{S_{xx}} + g_{yy}g_{S_{yy}} + g_{zz}g_{S_{zz}}}{3}\right] \quad (6)$$

Further simplification can be made for the case of an axially symmetric complex since $g_{xx} = g_{yy}$, thus

$$\left(\frac{\Delta H}{H}\right)^{D+L} = \frac{\beta^2 s'(s'+1)}{9kTR^3}(g_{\parallel}{}^2 - g_{\perp}{}^2)(1 - 3\cos^2\theta) \quad (7)$$

as reported for cobalt(II) complexes (27). Similarly, for axial symmetry, the Fermi contact equation is

$$\left(\frac{\Delta H}{H}\right)^{F} = -\frac{\beta s'(s'+1)A}{9\hbar\gamma_N kT}(g_{\parallel} + 2g_{\perp}) \quad (8)$$

In our experiments, the high spin ferrimyoglobin will be presumed to be axially symmetric since the low temperature EPR g values are $g_{\parallel} = 2$ and $g_{\perp} = 6$ (28, 29), but the assumption of no zero field splitting is clearly inappropriate. For Fe^{3+} ($s' = 5/2$) systems, there will be three Kramers doublets; thus, Equations 7 and 8 become (26)

$$\left(\frac{\Delta H}{H}\right)^{D+L} = \frac{\beta^2 s'(s'+1)}{9kTR^3}(1 - 3\cos^2\theta)(g_{\parallel}{}^2 - g_{\perp}{}^2) \cdot \left[1 - \frac{32(g_{\parallel}{}^2 + g_{\perp}{}^2/2)D}{15(g_{\parallel}{}^2 - g_{\perp}{}^2)kT}\right] \quad (9)$$

and

$$\left(\frac{\Delta H}{H}\right)^{F} = -\frac{\beta s'(s'+1)A}{9\hbar\gamma_N kT}(g_{\parallel} + 2g_{\perp})\left[1 - \frac{32(g_{\parallel} - g_{\perp})D}{15(g_{\parallel} + 2g_{\perp})kT}\right] \quad (10)$$

where $2D \simeq 20$ cm^{-1} (29) and $kT \sim 200$ cm^{-1} at room temperature. The new term thus introduces a small correction factor to the hyperfine shift expressions.

The above expressions give only a brief picture of the factors that may be significant in interpretation of the solid state ^{2}H NMR spectra of labeled hemeproteins, and the reader is referred to the literature for further discussion (25–27).

RESULTS AND DISCUSSION

As pointed out elsewhere (11), it is possible to determine the orientation of a particular ^{2}H-labeled group in a magnetically ordered system from its quadrupole splitting ($\Delta\nu_Q$) and a knowledge of the breadth of the random powder pattern distribution, *i.e.* electric quadrupole coupling constant, e^2qQ/h. However, it is difficult to obtain accurate powder pattern breadths of heme ^{2}H-labeled ferriaquomyoglobins due to the large overall spectral breadth and, more importantly, due to large deuteron paramagnetic shifts, resulting in "asymmetric" powder spectra. We have, therefore, measured the powder spectral breadths of the diamagnetic protoporphyrin IX dimethyl esters. The e^2qQ/h value found for the meso-deuterons was determined to be 195 kHz, slightly larger than the average e^2qQ/h = ~184 kHz found previously for aromatic deuterons (30), the e^2qQ/h values for the [*methylene*-6,7-*b*-$^2H_4$] deuterons and [*dimethyl*-1,3-$^2H_6$]deuterons being 162 kHz and 57 kHz, respectively (data not shown). A decrease by a factor of ~3 in the effective e^2qQ/h is expected for methyl deuterons if they are undergoing fast C_3 rotation, and the results with the aliphatic labeled species are consistent with those reported previously (30).

[Meso-α,β,γ,δ-$^2H_4$]heme-labeled Aquoferrimyoglobin—We show in Fig. 2 the ^{2}H NMR spectrum of [meso-α,β,γ,δ-$^2H_4$] heme-labeled aquoferrimyoglobin microcrystals suspended in ~90% saturated $(NH_4)_2SO_4$ at pH = 6.8, obtained by the Fourier transform method at 55.3 MHz (corresponding to a magnetic field strength of 8.5 Tesla). Four relatively sharp resonances (Fig. 2*A*, *a* to *d*) are observed from this magnetically ordered sample, and these peaks are shifted by +165 kHz (*a*), +53 kHz (*b*), −75 kHz (*c*), and −110 kHz (*d*) from

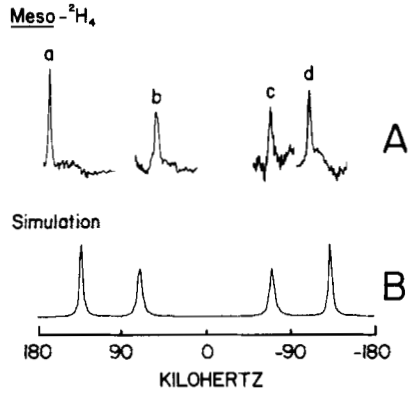

FIG. 2. **Deuterium quadrupole echo Fourier transform NMR spectra at 55.3 MHz and 25 °C of [meso-α,β,γ,δ-$^2H_4$]heme-labeled aquoferrimyoglobin from *P. catodon*, magnetically ordered in ~95% saturated $(NH_4)_2SO_4$, together with a computer simulation.** *A*, magnetically ordered spectrum taken in pieces, ~10^6 scans each spectrum at a 60-ms recycle time, $\tau_1 = \tau_2 = 55$ μs, 7 μs 90° pulse widths. *B*, simulation having $\Delta\nu_Q$ = 275 and 128 kHz and line widths of 2 kHz and 3 kHz, respectively.

the position of a diamagnetic meso-^{2}H-labeled heme in organic solvent. At first sight, there are a number of perhaps puzzling points about the result of Fig. 2*A*. First, there are only 4 peaks, not the 8 expected from 4 nonequivalent deuterons. Second, the peaks appear to have somewhat different intensities. Third, the 4 observed peaks are not symmetrically disposed about the diamagnetic, isotropic solution shift (0 kHz). These observations may be clarified by means of additional temperature dependence studies (see below) and by comparison with the theoretical predictions based on the high resolution x-ray crystal structure (31) as follows. First, only 4 peaks are seen since the (α, γ) and (β, δ) pairs are related by 180° and thus appear identical in the ^{2}H NMR experiment. Second, as discussed below, the differential peak heights likely originate in different line widths due to static disorder, rather than differential ^{2}H label incorporation (32), since our hemes contain 80 ± 5% ^{2}H at all four meso-sites. Third, the peaks are not expected to be symmetrically disposed about the Larmor frequency, ω_0, due to the large effect of the hyperfine shift due to the paramagnetic center. We explore these points as follows.

Using the crystallographic coordinates of Takano (31), we find that the angle between the c^* axis (oriented along H_0, Ref. 11) and the vector $\overrightarrow{CHD\ CHB}$ (Fig. 3) is 14.1° and the angle between c^* (H_0) and $\overrightarrow{CHC\ CHA}$ is 84.3°. The predicted ^{2}H NMR spectrum should thus consist of two pairs of splittings, one of $\Delta\nu_Q$ = 266 kHz and one of $\Delta\nu_Q$ = 142 kHz. Best agreement with the experimental result of Fig. 2*A* is obtained assuming peaks *a* and *d*, having $\Delta\nu_Q$ = 275 kHz, arise from $^2H^{\beta,\delta}$ and peaks *b* and *c*, having $\Delta\nu_Q$ = 128 kHz, arise from $^2H^{\alpha,\gamma}$. These tentative assignments are supported by analysis of the paramagnetic shift data and the temperature-dependent shift data discussed in the next section. The above results might also be interpretable in terms of some static disorder and perhaps librational motion about $C^{\beta,\delta}$ which could account for the larger discrepancy observed between theory and experiment for the $^2H^{\alpha,\gamma}$ quadrupole splitting and the apparently larger line widths of peaks *b* and *c* (decreased peak intensities in Fig. 2*A*), although this point is quite speculative.

Analysis of Hyperfine Shifts—The positions of peaks *a–d* in Fig. 2*A* are not symmetric about ω_0 as would be expected in the case of a diamagnetic molecule (11), and we show in Fig. 2*B* a computer-simulated magnetically ordered ^{2}H NMR spectrum having $\Delta\nu_Q$ = 275 and 128 kHz.

Paramagnetic shift measurements in solution using ^{1}H

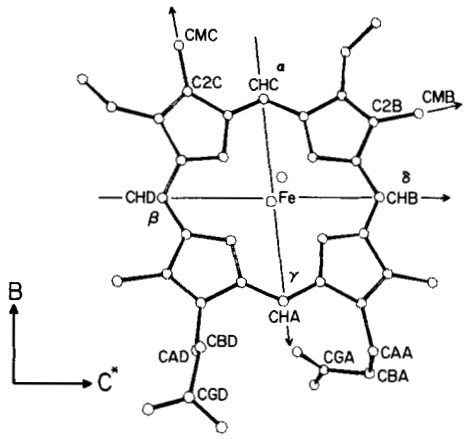

FIG. 3. **Computer drawing of the heme macrocycle in *P. catodon* aquoferrimyoglobin showing the angular relationship between sites of deuterium labeling and the crystallographic axes.** Crystallographic data were those of Takano (31), as supplied by the Brookhaven protein crystal data bank.

NMR are well documented for both model hemes and in hemeproteins themselves (32–37). The origin of the paramagnetic shift is due either to magnetic anisotropy, or to transferred spin density, or a combination of both effects. The former gives rise to a dipolar shift characterized by $(\Delta H/H)^{D+L}$ and the latter to the Fermi contact shift characterized by $(\Delta H/H)^{F}$. The Fermi contact shift is not orientation-dependent, while the dipolar shift is (see above). From our results (Fig. 2*A*), it is clear that our shift is definitely orientation-dependent. For $^2H^{\beta,\delta}$, the midpoint of the splitting of resonances *a* and *d* is +27.5 kHz from the zero frequency, while the center frequency shift for $^2H^{\alpha,\gamma}$ (peaks *b* and *c*) is −11 kHz. The errors on these shifts are ~1–2 kHz. Therefore, the dipolar term dominates the paramagnetic shift experienced by the meso-deuterons in aquoferrimyoglobin crystals, and a similar conclusion has been reached for protons in solution NMR studies (38). However, direct substitution into Equation 7 under "Theoretical Aspects" implies an equal field shift for all four meso-deuterons, with a smaller magnitude than that observed, since all meso-deuterons are at right angles to the symmetry axis of the heme. This apparent discrepancy is due to the fact that Equation 7 is strictly only applicable to *isotropic* hyperfine shifts. A more general form of Equation 7 can be found in Ref. 39 and is

$$\Delta H/H\,(\theta,\Omega) = -\frac{\beta^2 s'(s'+1)}{3kTR^3}\Big\{g_{\parallel}{}^2\cos^2\theta(3\cos^2\chi - 1) + g_{\perp}{}^2\sin^2\theta(3\sin^2\chi\cos^2\Omega - 1) + \frac{3}{4}(g_{\parallel}{}^2 + g_{\perp}{}^2)\sin 2\theta\sin 2\chi\cos\Omega\Big\} \quad (11)$$

where R is the distance of the nucleus from the paramagnetic center (assumed to be the Fe^{3+} ion), χ is the angle between the symmetry axis and R, θ gives the orientation of the symmetry axis relative to the field direction (H_0), and Ω describes the rotation about the symmetry axis.

In the case of our ^{2}H-labeled magnetically ordered aquoferrimyoglobin microcrystal sample, the magnetic field H_0 is oriented *approximately* perpendicular to the heme normal (11). We may, therefore, carry out a back of the envelope calculation of the sign and relative magnitudes of the $^2H^{\beta,\delta}$ and $^2H^{\alpha,\gamma}$ hyperfine shifts as follows. For $^2H^{\beta,\delta}$, $\theta = 90°$, $\chi = 90°$, and $\Omega = 14.1°$. Substituting into Equation 12 thus gives

$$\Delta H/H \simeq -\frac{\beta^2 s'(s'+1)}{3kTR^3}[g_{\perp}{}^2(3\cos^2\Omega - 1)] \simeq -\frac{\beta^2 s'(s'+1)g_{\perp}{}^2}{3kTR^3}(1.824) \quad (12)$$

For $^2H^{\alpha,\gamma}$, $\theta = 90°$, $\chi = 90°$, $\Omega = 84.3$ and 95.7°, and the predicted shift is

$$\Delta H/H \simeq -\frac{\beta^2 s'(s'+1)}{3kTR^3}[g_{\perp}{}^2(3\cos^2\Omega - 1)] \simeq +\frac{\beta^2 s'(s'+1)g_{\perp}{}^2}{3kTR^3}(0.9704) \quad (13)$$

The above results clearly indicate that the predicted shifts for $^2H^{\beta,\delta}$ are about *twice* those of $^2H^{\alpha,\gamma}$ (observed +27.5 kHz and −11.0 kHz) and are also *of opposite sign*. The lower field shift of $^2H^{\beta,\delta}$ correlates with the higher frequency shift observed experimentally (Fig. 2*A*). The difference between the observed and calculated shift ratios may be a reflection of a small contribution from the Fermi contact term, in addition to the approximations used.

An important point to note at this point is that the hyperfine shifts observed are very large, for example, a 27.5-kHz shift at 55.3 MHz corresponds to some 500 ppm! This value is an order of magnitude larger than the shift of meso-protons of aquoferrimyoglobin measured by ^{1}H NMR spectroscopy (37) since in solution we see a hyperfine shift averaged by particle tumbling. The isotropic rotational motion of the protein has a correlation time $\sim 10^{-7}$–10^{-8} s and results in an effective averaging of the $\sim 10^4$ Hz hyperfine anisotropy seen in Fig. 2*A*. Again, an approximate calculation serves to link the solid and solution state NMR observations as follows.

If we assume that the anisotropic shift in the solid may be expressed as in Equation 11 and the isotropic shift in the solid by Equation 7, there exists a ratio of ~6 between them. Then, a value of ~500/6 = 83 ppm may be determined for the isotropic shift in the solid. Since we also know the ratio of isotropic shifts in the solid to that in solution is $\sim 3(g_{\parallel} + g_{\perp})/(g_{\parallel} + 2g_{\perp})$ (39) or ≈1.71, we may estimate a solution isotropic shift of 83 ÷ 1.71 or ≈48 ppm. Solution isotropic hyperfine shifts of a variety of high spin ferric hemoproteins and model complexes are ≈40 ppm (33, 37), suggesting good agreement between solution and crystal results although our use of low temperature *g* values may be questionable.

Temperature Dependence of Paramagnetic Shifts—As outlined in Equations 7, 8, and 11, the general test for a paramagnetic shift is that it be αT^{-1}. We have, therefore, obtained ^{2}H Fourier transform NMR spectra of [meso-$\alpha,\beta,\gamma,\delta$-$^2H_4$] heme-labeled magnetically ordered aquoferrimyoglobin microcrystals at −60 °C, −25 °C, 25 °C, and 49 °C, and the Curie plots of T^{-1} *versus* frequency are given in Fig. 4. The plots of Fig. 4 are all linear and at infinite temperature ($1/T = 0$) give rise to an essentially symmetric magnetically ordered ^{2}H NMR spectrum. In addition, the results of Fig. 4 show clearly that peaks *a* and *d* arise from the same deuteron pair ($^2H^{\beta,\delta}$), and peaks *b* and *c* arise from the other deuteron pair ($^2H^{\alpha,\gamma}$) since the magnitudes and signs of the slopes, respectively (*a* and *d*) (*b* and *c*), are clearly correlated (Fig. 4). Such correlations may be made in the absence of any crystallographic data, facilitating spectral assignment and the derivation of structural information.

[Methylene-6,7-b-$^2H_4$]heme-labeled Aquoferrimyoglobin—We show in Fig. 5 the ^{2}H NMR spectrum of a magnetically ordered sample of [*methylene*-6,7-*b*-$^2H_4$]heme-labeled aquoferrimyoglobin. Signals, with different intensities, are observed at about +70 kHz (*e*), +50 kHz (*f*), +40 kHz (*g*), −40 kHz (*h*), −50 kHz (*i*), and −70 kHz (*j*) with respect to the zero frequency (0 kHz), strongly suggesting the lack of any appreciable hyperfine shifts due to the considerable distance of the *b*-CH_2 groups from the paramagnetic center (r^3 *and* θ dependence). This is supported by the results of solution ^{1}H NMR studies on high spin Fe^{3+} complexes where the paramagnetic [*methylene*-6,7-*b*-$^1H_4$]heme proton shifts were

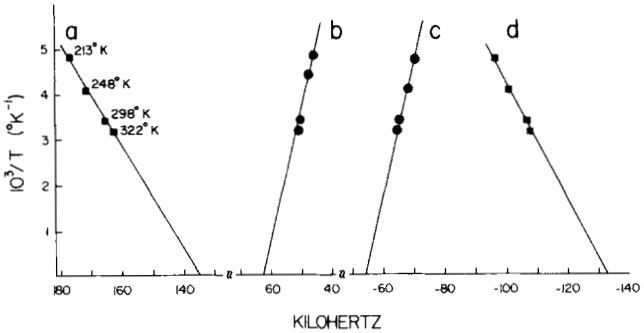

FIG. 4. Plot of resonance position *versus* the reciprocal of the absolute temperature for meso-^{2}H-labeled aquoferrimyoglobin microcrystals (peaks *a–d* of Fig. 2*A*), showing that *peaks a* and *d*, *b* and *c* are correlated.

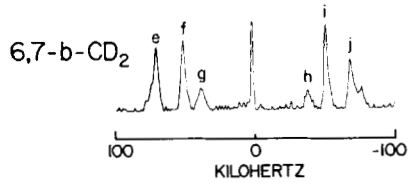

FIG. 5. **Fifty-five MHz deuterium quadrupole echo Fourier transform NMR spectrum at 25 °C of magnetically ordered [*methylene*-6,7-*b*-^{2}H$_4$]heme-labeled *P. catodon* aquoferrimyoglobin microcrystals.** 131,072 scans, 105-ms recycle time, $\tau_1 = \tau_2 = 55$ μs, 2.5 μs 90° pulse widths, ± 500 kHz spectral width, 4,096 real data points, line broadening = 500 Hz.

shown to be less than one-tenth those of the protons (33). For the present case, this would represent a ~1–3 kHz shift, which is close to our experimental error.

The results of Fig. 5 also suggest a lack of any fast large amplitude *b*-methylene group motions. If there were fast rotation about either of the propionate C-C σ bonds proximal to the heme, then the observed splitting in a magnetically ordered system could not exceed ~80 kHz. However, we observe resonances having splittings considerably in excess of this (Fig. 5), indicating "locked" propionic acid side chains. The x-ray crystallographic results (31) indicate that both propionates are involved in two hydrogen-bonding interactions. The carboxyl of side chain 7 is bonded to His 2FG of the same molecule and to Gln 5H of a neighboring one, while the carboxyl of side chain 6 is bonded to Arg 3CD and a solvent molecule. The presence of these hydrogen bonds may be the cause of the apparent immobility of the two adjacent methylene residues in the solid state ^{2}H NMR spectrum (Fig. 5).

We shall now attempt to interpret the results of Fig. 5, but first, we would like to point out that studies of an unknown crystal system would clearly require synthesis of selectively labeled, chiral, 6 and 7-methylene-^{2}H$_1$-labeled species, in which case considerable static and dynamic side chain structural information should become available. Since this would be the topic of a separate study, we shall thus indicate how we may assign the crystal spectra by use of the crystallographic coordinates. We first calculate the deuteron positions using the coordinates of atoms CAA, CBA, CGA, CAD, CBD, and CGD in Fig. 3 together with an assumed HCH bond angle of 140°, based on the x-ray crystal structure of adipic acid (40–42). Some arithmetic then yields angles θ' between the C-^{2}H vectors and H_0 (the crystallographic c^* axis) of 76°, 40°, 135°, and 34°, corresponding to $\Delta\nu_Q = 99$, 93, 61, and 129 kHz. These splittings are in moderate agreement with those observed (102, 102, 75, and 138 kHz) if we assume peaks *f* and *i* are each 1-deuteron resonances and peaks *e*, *g*, *h*, and *j* are 0.5-deuteron resonances, respectively, and better agreement is obtained if e^2qQ/h is taken to be somewhat larger than 162 kHz. Differential spin lattice relaxation and line widths (due to some static or limited dynamic disorder or to relaxation) and spin echo refocusing effects may all in principle contribute to spectral intensity distortions, as may nonuniformities in ^{2}H labeling. Consequently, these results should be considerably improved upon by synthesis of the appropriate individually labeled 6- or 7-*b*-methylene species (or their R or S forms), but this is clearly no mean synthetic task. Interestingly, a difference in line width of the two *b*-hydrogen resonances is also observed in the ^{1}H NMR of aquoferrimyoglobin in solution (37).

We should also add that an alternative possibility for the intensity anomaly, and shoulders of peaks *e* and *j*, is that there are two conformations for both the 6-*b*- and the 7-*b*-methylene residues. Again, selective labeling appears necessary to clarify this point. We find that good agreement with the experimental intensities and close agreement with the experimental splittings may be obtained by assuming two approximately equally populated conformers for the 6-*b* and 7-*b* sites, in which the rotamer angle is about 120°. The peak splittings, intensities, and angles (between the C-^{2}H vector and the c^* axis) are: 6-*b*: conformer A, 61 kHz ($\frac{1}{2}$) 135°, 129 kHz ($\frac{1}{2}$) 34°; conformer B, 110 kHz ($\frac{1}{2}$) 100°, 129 kHz ($\frac{1}{2}$) 34°; and 7-*b*: conformer A, 99 kHz ($\frac{1}{2}$) 76°, 93 kHz ($\frac{1}{2}$) 40°; conformer B, 99 kHz ($\frac{1}{2}$) 76°, 150 kHz ($\frac{1}{2}$) 150°.

[Methyl-1,3-^{2}H$_6$]heme-labeled Aquoferrimyoglobin—The spectrum of Fig. 6*A* originates from a heme containing about 80% ^{2}H in the 1,3-methyls and about 100% ^{2}H in the 6,7-*b*-methylenes. That of Fig. 6*B* contains about 80% ^{2}H in the 1,3-methyls and was from a sample in which the 6,7-*b*-methylene deuteron component had been reduced by back exchange of the heme during synthesis. Clearly, peaks *e*, *f*, *g*, *h*, *i*, and *j* in Fig. 6*A* arise from these methylene deuterons (see Fig. 5*A*). Therefore, peaks *k*, *l*, *m*, and *n* in Fig. 6, *A* and *B*, originate primarily from the [*methyl*-1,3-^{2}H$_6$]heme deuterons, the difference spectrum of Fig. 6*C* being close to that of the methylene-labeled species (Fig. 5*A*). Similar conclusions may be drawn from a spectrum of a 50% ^{2}H-methyl-labeled species (data not shown).

Note that peaks *k*, *l*, *m*, and *n* of Fig. 6, *A* and *B*, are not symmetrically disposed about 0 kHz due to the presence of hyperfine effects, as observed previously with the meso-deu-

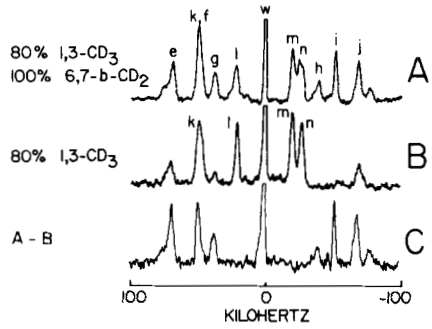

FIG. 6. **Fifty-five MHz deuterium quadrupole echo Fourier transform NMR spectra at 25 °C of [*methyl*-1,3-^{2}H$_6$] and [*methyl*-1,3-^{2}H$_6$; *methylene*-6,7-*b*-^{2}H$_4$]heme-labeled magnetically ordered aquoferrimyoglobin crystals.** *A*, spectrum of double-labeled species which contained ~80% 1,3-CD$_3$, 100% 6,7-b-CD$_2$ label, 262,144 scans, 105-ms recycle time, $\tau_1 = \tau_2 = 55$ μs, 3.5 μs 90° pulse widths, ±250 kHz spectral width, 4,096 real data points, line broadening = 500 Hz. *B*, spectrum of 80% 1,3-CD$_3$ label, 262,144 scans, 105-ms recycle time, $\tau_1 = \tau_2 = 55$ μs, 2.5 μs 90° pulse widths, ±250 kHz spectral width, 4,096 real data points, line broadening = 500 Hz. *C*, *A–B*.

terons. The resonance frequencies are +50 kHz, +21.5 kHz, −19.2 kHz, and −26.9 kHz for peaks *k*, *l*, *m*, and *n*, respectively. Assuming a quadrupole coupling constant e^2qQ/h = 57 kHz (30), we obtain the result that the angles (θ') between the C_3 axes of the heme methyl groups are 14.6° and either 83.3 or 96.7° (Table I). Since the heme geometry is known and the heme orientation has been deduced above, the possible solutions are θ' = 14.6° and 96.7°. Selective deuteration would enable a specific assignment, although, of course, it must be realized that even specific labeling does not solve the NMR "phase problem," and that for the general case, there will be either four or eight vector orientations for a given $\Delta\nu_Q$ measurement. For example, in the present case, a $\Delta\nu_Q$ = 41 kHz yields θ' = ±83.3° or ±96.7°. For the $H^{\alpha,\gamma}$ vector orientation ($\Delta\nu_Q$ = 128 kHz) θ' = ±38.5°, ±77.9°, ±102.1°, or ±141.5°, *i.e.* there are eight solutions, and multiple labeling experiments are required in order to reduce this number. The minimum will, however, still be four solutions since NMR cannot determine "up" from "down" or "left" from "right," but in the present case, two sets of solutions will arise in any case since there are two molecules in the unit cell.

In any case, inspection of the x-ray data indicates that peaks *k* and *n* arise from the 1-methyl group and peaks *l* and *m* arise from the 3-methyl group. The angle between the $\overrightarrow{C2B\ CMB}$ (1-Me) vector and c^* being 15.8°, close to the 14.9° solution noted above, and that of the $\overrightarrow{C2C\ CMC}$ (3-Me) vector and c^* being 101.6°, close to the 96.7° solution found from the NMR results (Table I).

As noted above the positions of resonances *k*, *l*, *m*, and *n* in Fig. 6 are not symmetric with respect to the zero frequency, indicating a considerable contribution from paramagnetic shift effects, as seen previously with the meso-heme-labeled species (Fig. 2). An approximate point-dipole calculation serves to check if the observed shifts are of the magnitude expected in the crystalline solid state. First, we shall assume dominance of the dipolar term, as in the case of meso-deuterons. Since the methyl deuterons are about 6.5 Å from the Fe^{3+} center, while the meso-deuterons are about 4.5 Å away, and $(\Delta H/H)^{D+L}$ is proportional to R^{-3}, distance effects will reduce the dipolar shift by a factor of ≈3. The geometric factor for the 1-CD_3 group is nearly identical with that of the β and δ meso-deuterons; therefore, its shift is expected to have the same sign, *i.e.* it should occur at about 27.5/3 = 9.2 kHz to higher frequency. Based on the same reasoning, the 3-CD_3 group should resonate ~3.7 kHz to lower frequency. Experimentally, as shown in Fig. 6, *A* and *B*, we observe an ~+12 kHz shift for the 1-CD_3 group but only about a −1 kHz shift (within our experimental error) for the 3-CD_3 group. If the Fermi contact term cannot be neglected in this case, and both σ and π delocalization produce a downfield shift (43, 44), we can rationalize the experimental result by assuming a downfield Fermi contact shift of about 3 kHz for both the 1 and 3-CD_3 groups. If this hypothesis is correct, then in solution, the overall shift based on the calculation done previously for the meso-labeled species would be ≈4.2 kHz, equivalent to ≈75 ppm. The shifts for 1,3-CH_3 groups in aquoferrimyoglobin in solution are 73 and 53 ppm as measured by solution ^1H NMR (37), close to the predicted value. Although very crude, these calculations, together with those discussed above for the [meso-α, β, γ, δ-$^2H_4$]heme-labeled aquoferrimyoglobin, give very good agreement between solid state and solution hyperfine shifts and, perhaps more importantly, emphasize the very great magnitude of the shifts seen in paramagnetic solids.

Concluding Remarks—The results presented in this paper represent our first attempt at detailing the organization of a heme residue in a hemoprotein in the crystalline solid state using ^2H NMR spectroscopic methods. Our results indicate that in the solid state, extremely large magnetic hyperfine shifts (100's to perhaps 1000's of ppm) will, in general, be seen for nuclei close to paramagnetic centers. However, even though their individual line widths may be several thousands of Hertz, they may be readily detected using high field Fourier transform pulse methods. Solid state shifts may be an order of magnitude larger than those seen in solution. Our results clearly indicate the dominance of dipolar rather than Fermi contact shifts in the solid state. Overall, our results give excellent agreement between ^2H NMR and x-ray crystallographic determinations of heme organization. The NMR experiments are quite rapid, but suffer from uncertainties of $\pi/2$, π, or $3\pi/2$ in the orientations of a given C-^2H vector and only give information on those groups that have been labeled.

A complete summary of the x-ray and ^2H NMR-derived structural parameters is given in Table I.

TABLE I

Assignment of ^2H NMR resonances in meso, 6,7-methylene and 1,3-methyl-labeled aquoferrimyoglobin crystals, at 23 °C, and comparison of NMR and x-ray-derived structural parameters

Data were obtained by the Fourier transform method at a magnetic field strength of 8.5 Tesla (corresponding to a ^2H resonance frequency of 55.3 MHz), using the results of Figs. 2, 4, 5, and 6 and additional unpublished data. The protein microcrystals were suspended in ~95% saturated $(NH_4)_2SO_4$ and were all magnetically ordered.

Deuterium label[a]	Quadrupole splitting ($\Delta\nu_Q$)[b]	Theoretical angle (θ')[c]	Experimental angle (θ')[d]	Paramagnetic shift[e]
	kHz			*ppm*
α,γ-Meso	128	84.3°	77.9°	−200
β,δ-Meso	275	14.1°	11.5°	+500
6-*b* Methylene				
Conformer A	138 (½)	34.0°	32.5°	~0
	75 (½)	135.0°	137.3°	~0
Conformer B	138 (½)	34.0°	32.5°	~0
	100 (½)	100.0°	103.4°	~0
7-*b* Methylene				
Conformer A	102 (½)	75.6°	76.6°	~0
	102 (½)	40.4°	38.5°	~0
Conformer B	102 (½)	75.6°	76.6°	~0
	150 (½)	150.0°	149.6°	~0
1-Methyl	77	15.8°	14.6°	+220
3-Methyl	41	101.6°	96.7°	−19

[a] ^2H-labeled hemes were prepared by chemical synthesis and incorporated into apomyoglobin as discussed under "Experimental Procedures." Crystals were in the range of ~0.01–0.1-mm long prisms.

[b] Peak to peak separation; the error is ±1–2 kHz.

[c] Obtained from the coordinates of Takano (31) for myoglobin and Housty and Hospital (Refs. 40–42) for the HCH angle in the model system adipic acid (*b*-methylenes of propionate).

[d] The errors are up to ~ ± 3°. Quadrupole coupling constants were 195 kHz (meso), 162 kHz (*b*-methylene), or 57 kHz (methyl); η assumed = 0.

[e] The error is about ±20 ppm. Negative shifts are to lower frequency (higher field; $\Delta H/H$ positive).

Acknowledgments—We thank Ben Montez for help with protein isolation and reconstitution and Tane Ray and Ross Simpson for help with computer graphics.

REFERENCES

1. Blundell, T. L., and Johnson, L. N. (1976) *Protein Crystallography*, Academic Press, NY
2. Dwek, R. A. (1973) *Nuclear Magnetic Resonance in Biochemistry: Applications to Enzyme Systems*, Clarendon Press, Oxford
3. Campbell, I. D., Dobson, C. M., and Williams, R. J. P. (1975) *Proc. R. Soc. Lond., Ser. A* **345**, 23–40
4. Oldfield, E., Norton, R. S., and Allerhand, A. (1975) *J. Biol. Chem.* **250**, 6381–6402
5. Wüthrich, K. (1976) *NMR in Biological Research: Peptides and*

Proteins, American Elsevier, Inc., NY
6. Gurd, F. R. N., and Rothgeb, T. M. (1979) *Adv. Protein Chem.* **33,** 73–165
7. Williams, R. J. P. (1978) *Proc. R. Soc. Lond., Ser. B* **200,** 353–389
8. Frauenfelder, H., Petsko, G. A., and Tsernoglou, D. (1979) *Nature* **280,** 558–563
9. Artymiuk, P. J., Blake, C. C. F., Grace, D. E. P., Oatley, S. J., Phillips, D. C., and Sternberg, M. J. E. (1979) *Nature* **280,** 563–568
10. Oldfield, E., and Rothgeb, T. M. (1980) *J. Am. Chem. Soc.* **102,** 3635–3637
11. Rothgeb, T. M., and Oldfield, E. (1981) *J. Biol. Chem.* **256,** 1432–1446
12. Oldfield, E., Janes, N., Kinsey, R., Kintanar, A., Lee, R. W. K., Rothgeb, T. M., Schramm, S., Skarjune, R., Smith, R., and Tsai, M-D. (1981) *Biochem. Soc. Symp.* **45,** 155–181
13. Kenner, G. W., Smith, K. M., and Sutton, M. J. (1973) *Tetrahedron Lett.* **16,** 1303–1306
14. Cavaleiro, J. A. S., Gonsalves, A. M. d'A. R., Kenner, G. W., and Smith, K. M. (1974) *J. Chem. Soc. Perkin Trans. I* 1771–1781
15. Janson, T. R., and Katz, J. J. (1972) *J. Mag. Res.* **6,** 209–220
16. Evans, B., Smith, K. M., La Mar, G. N., and Viscio, D. B. (1977) *J. Am. Chem. Soc.* **99,** 7070–7072
17. Smith, K. M., Eivazi, F., Langry, K. C., De Almeida, J. A. P. B., and Kenner, G. W. (1979) *Bioorg. Chem.* **8,** 485–495
18. Adler, A. D., Longo, F. R., Kampas, F., and Kim, J. (1970) *J. Inorg. Nucl. Chem.* **32,** 2443–2445
19. Wüthrich, K., Shulman, R. G., Wyluda, B. J., and Caughey, W. S. (1969) *Proc. Natl. Acad. Sci. U. S. A.* **62,** 636–643
20. Hapner, K. D., Bradshaw, R. A., Hartzell, C. R., and Gurd, F. R. N. (1968) *J. Biol. Chem.* **243,** 683–689
21. Rothgeb, T. M., and Gurd, F. R. N. (1978) *Methods Enzymol.* **52,** 473–486
22. Kendrew, J. C., and Parrish, R. G. (1956) *Proc. R. Soc. Lond., Ser. A* **238,** 305–324
23. Oldfield, E., Meadows, M., Rice, D., and Jacobs, R. (1978) *Biochemistry* **17,** 2727–2740
24. Davis, J. H., Jeffrey, K. R., Bloom, M., Valic, M. I., and Higgs, T. P. (1976) *Chem. Phys., Lett.* **42,** 390–394
25. Kurland, R. J., and McGarvey, B. R. (1970) *J. Mag. Res.* **2,** 286–301
26. Jesson, J. P. (1973) in *NMR of Paramagnetic Molecules* (LaMar, G. N., Horrocks, W. D., Jr., and Holm, R. H., eds) pp. 1–52, Academic Press, New York
27. Jesson, J. P. (1967) *J. Chem. Phys.* **47,** 579–581; 582–591
28. Hori, H. (1971) *Biochim. Biophys. Acta* **251,** 227–235
29. Slade, E. F., and Farrow, R. H. (1972) *Biochim. Biophys. Acta* **278,** 450–458
30. Brevard, C., and Kintzinger, J. P. (1978) in *NMR and the Periodic Table* (Harris, R. K., and Mann, B. E., eds) p. 119, Academic Press, New York
31. Takano, T. (1977) *J. Mol. Biol.* **110,** 537–568
32. La Mar, G. N., Viscio, D. B., Smith, K. M., Caughey, W. S., and Smith, M. L. (1978) *J. Am. Chem. Soc.* **100,** 8085–8092
33. Budd, D. L., La Mar, G. N., Langry, K. C., Smith, K. M., and Nayyir-Mazhir, R. (1979) *J. Am. Chem. Soc.* **101,** 6091–6096
34. La Mar, G. N., Overkamp, M., Sick, H., and Gersonde, K. (1978) *Biochemistry* **17,** 352–361
35. La Mar, G. N., Viscio, D. B., Gersonde, K., and Sick, H. (1978) *Biochemistry* **17,** 361–367
36. Shulman, R. G., Glarum, S. H., and Karplus, M. (1971) *J. Mol. Biol.* **57,** 93–115
37. La Mar, G. N., Budd, D. L., Smith, K. M., and Langry, K. C. (1980) *J. Am. Chem. Soc.* **102,** 1822–1827
38. La Mar, G. N., and Walker, F. A. (1973) *J. Am. Chem. Soc.* **95,** 1782–1790
39. McConnell, H. M., and Robertson, R. E. (1958) *J. Chem. Phys.* **29,** 1361–1365
40. Housty, J., and Hospital, M. (1965) *Acta Cryst.* **18,** 693–697
41. Housty, J., and Hospital, M. (1966) *Acta Cryst.* **20,** 325–329
42. Housty, J., and Hospital, M. (1966) *Acta Cryst.* **21,** 553–559
43. Kurland, R. J., Little, R. G., Davis, D. G., and Ho, C. (1971) *Biochemistry* **10,** 2237–2246
44. LaMar, G. N. (1973) in *NMR of Paramagnetic Molecules* (LaMar, G. N., Horrocks, W. D., Jr., and Holm, R. H., eds) pp. 85–126, Academic Press, New York